**Geomechanics and Engineering**, *Vol. 32, No. 5 (2023) 523-540*
https://doi.org/10.12989/gae.2023.32.5.523


# Comprehensive evaluating the stability of slope reinforced with free and fixed head piles

Xixi Xiong[1], Ying Fan*[1], Jinzhe Wang[1] and Pooya Heydari[2]

[1]*College of Civil Engineering, Architecture and Environment, Hubei University of Technology, Wuhan, Hubei Province 430068, China*
[2]*Department of Geotechnical engineering, Moghadas Ardabili Institute of Higher Education, Ardabil, Iran*

(*Received August 24, 2022, Revised February 13, 2023, Accepted February 15, 2023*)

**Abstract.** The failure of slope can cause remarkable damage to either human life or infrastructures. Stabilizing piles are widely utilized to reinforce slope as a slip-resistance structure. The workability of pile-stabilized slopes is affected by various parameters. In this study, the performance of earth slope reinforced with piles and the behavior of piles under static load, by shear reduction strength method using the finite difference software ($FLAC^{3D}$) has been investigated. Parametric studies were conducted to investigate the role of pile length ($L$), different pile distances from each other ($S/D$), pile head conditions (free and fixed head condition), the effect of sand density (loose, medium, and high-density soil) on the pile behavior, and the performance of pile-stabilized slopes. The performance of the stabilized slopes was analyzed by evaluating the factor of safety, lateral displacement and bending moment of piles, and critical slip mechanism. The results depict that as $L$ increased and $S/D$ reduced, the performance of slopes stabilized with pile gets better by raising the soil density. The greater the amount of bending moment at the shallow depths of the pile in the fixed pile head indicates the effect of the inertial force due to the structure on the pile performance.

**Keywords:** 3D numerical analysis; free and fixed head pile; $FLAC^{3D}$; pile-slope system; shear strength reduction method

## 1. Introduction

The social and economic damage caused by slope failure is high and increasing because the built spaces in the hillside areas expand due to the rising population (Fan *et al.* 2018, Esmaeili-Choobar *et al*. 2013). Slopes with angles larger than stability angle ($\varphi$) need additional passive forces (Esmaeili-Falak and Hajialilue-Bonab 2012). Mentioned forces could be supplied by vertical or horizontal reinforcing elements (Demerdash 1996, Moradi *et al.* 2022, Esmaeili Falak and Sarkhani Benemaran 2022). Exposure the crest of slope to the vertical force of the buildings either declines soil bearing capacity or raises the failure possibility of the slope, leading to the factor of safety ($FOS$) reduction (Ausilio *et al.* 2001). Seismic stability analysis of slopes reinforced with piles were analyzed employing shaking table tests and finite-element limit analysis (Li and Xiao 2022, Fang Pai *et al.* 2022, Fang Pai and Gang Wu 2021, Peng *et al.* 2022).

Various techniques, such as installing piles on the slopes, have been developed to stabilize the slope (Briançon and Simon 2012). To prevent landslides, stabilizing piles are widely utilized to enhance the stability of the slope (Gao *et al.* 2013). The advantage of slope stabilization with piles in comparison with encased granular columns and stone columns is their larger lateral bearing capacity because of their non-subsidence, non-weakness, and non-deformation under vertical load. The pile stabilization technique supplies the group treatment via concrete walls and is utilized in various kinds of soils. Other techniques can improve the liquefaction property during cyclic loading because of its drainage capability; however, this feature could be provided using a drainage pipe along with the pile (Mohapatra *et al.* 2016, Esmaeili-Falak *et al.* 2018).

In various geotechnical issues, piles are tolerated the lateral loads (Poorjafar *et al.* 2022). Depending on their application in practice, laterally loaded piles may be called passive or active. An active pile is mainly loaded on top to support a superstructure, such as a bridge. On the other hand, a passive pile, because of ground pressure, the load is employed mainly along its length. Using piles for stabilizing slopes is a passive loading occasion (Reese and Van Impe 2000). Evaluating and designing the passive piles in slopes is strenuous because of the complexity of the treatment of piles. Several stabilization analyses have been performed recent years, such as on homogeneous Slope Reinforced by Anti-Slide Piles (Xu *et al.* 2022), slope-stabilisation system combining gabion-faced geogrid-reinforced retaining wall with embedded piles (Wang *et al.* 2022), and finite soil slope in front of piles in landslide (Jiang *et al.* 2022).

Several analytical, experimental, and numerical techniques have been shown so as to assess the workability of the piles for slope stabilization. In general, mentioned techniques could be categorized into two categories, pressure or displacement-based techniques (Beer and Wallays 1972, Chen and Poulos 1997, Hassiotis *et al.* 1997, Hull *et al.* 1991, Ito and Matsui 1975, Harry 1995,

*Corresponding author, Ph.D.
E-mail: hbut2022@163.com
[a]Ph.D.



ISSN: 2005-307X (Print), 2092-6219 (Online)

Tschebotarioff 1973, Viggiani 1981), and numerical methods (Cai and Ugai 2000, Chow 1996, Goh *et al.* 1997, Jeong *et al.* 2003, Oakland and Chameau 1984, Poulos and Chen 1997, Wei and Cheng 2009, Won *et al.* 2005, Yang *et al.* 2011). In addition to numerical, analytical, and experimental procedures in engineering fields, the methods based on artificial intelligence also extended (Shi *et al.* 2023, Ge *et al.* 2022, Esmaeili-Falak *et al.* 2019, Aghayari Hir *et al.* 2022). Within the first category (i.e., pressure or displacement-based techniques), the pile is tolerated as an assumed slope movement. Within the first category (i.e., pressure- or displacement-based techniques), the pile is tolerated as an assumed slope movement. This, along with the distribution of the soil modulus with depth and the values of the mass contact pressure with the soil, must be determined in advance. Within the numerical technique, the issue is evaluated using the finite difference method (FDM) or the finite element method (FEM). Mentioned techniques could solve the whole 3D issue, considering the precise geometry, pile-soil interaction, and pile group impacts (Kourkoulis *et al.* 2011).

In former decades, the shear strength reduction method ($SSRM$) has been applied in the numerical analysis of slopes due to its advantages in solving slope stability problems. But, more considerations to the mesh design are needed with a soft limit or greatly intricated issues. Hence, more time for a solution is requisite to accomplish the $SSRM$ (Wei and Cheng, 2009). The mentioned technique has been utilized in the evaluation of the non-stabilized slopes (Alemdag *et al.* 2014, Cheng *et al.* 2007, Dawson *et al.* 1999, Donald and Giam 1988, Fahimifar *et al.* 2014, Griffiths and Lane 2001, Matsui and San 1992, Naylor 1982, Sarkar *et al.* 2012, Singh *et al.* 2013, Ugai and Leshchinsky 1995, Wei *et al.* 2009, Zienkiewicz *et al.* 1975) and stabilized slopes (Cai and Ugai 2000, Wei and Cheng 2009, Won *et al.* 2005, Yang *et al.* 2011).

Moreover, other studies analyzed the performance of pile-stabilized slopes by performing analytical and experimental methods together (Hajiazizi *et al.* 2017, 2018, Lei *et al.* 2021, Sharafi and Sojoudi 2016, Shooshpasha and Amirdehi 2015). The stability analysis of slope stabilized with one row of free head piles was analyzed by $SSRM$ with FEM method. The impacts of pile location, length, spacing, and bending stiffness were analyzed. The length of the critical pile, after which the $FOS$ remains constant, depends on the pile distance, the bending stiffness, and the angle of slope. The results depicted that the $FOS$ raises with reducing pile spacing and increasing bending stiffness (Lei *et al.* 2021). The paper created a slope and produced slope analysis reinforced by single- and double-row of piles in various spaces from slope toe by $FDM$. Considering $FOS$, it could be resulted that the optimal position for single-row and double-row stabilizing piles is at the slope's lower-middle and at the lower and lower-middle parts of the slope, respectively (Lei *et al.* 2021). An article presented the results of experimental and numerical models for the treatment of layered pile-stabilized slopes. The goal was to specify the optimal positioning of pile rows about parameters affecting the answer. Results presented that in slopes stabilized with two rows of piles, utilizing one of the rows in the location of the toe or crest, or utilizing these locations simultaneously, were rejected. As a conclusion, the coupling effect of piles row space ($L_p$)–pile location and size of soil grains also dramatically affect the optimum positioning of piles, so that increment in $\phi$ in greater $L_p$ causes to an optimized design (Sarkhani Benemaran *et al.* 2021).

According to the published articles, several significant geometric and physical variables that affect the usefulness of pile-stabilized slopes exist, named location of piles, length of piles, spacing of piles, the stiffness of piles, the condition of pile head, and mechanical properties of soil in slope. Based on the reported evaluations on many cases, the head of piles-stabilized slopes was free (Davies *et al.* 2003, Fukumoto 1972, 1976, Fukumoto 1975, Fukuoka 1977, Polysou *et al.* 1998, Yamin 2007, Zeng and Liang 2002). Hence, in this study, along with slopes with free head piles, slopes with fixed head piles were also created and analyzed by the $SSRM$ using the finite difference software ($FLAC^{3D}$) under static loaded. After that, parametric studies were conducted to investigate the role of pile length ($L$), different pile distances from each other ($S/D$), pile head conditions (free and fixed head condition), the effect of sand density (loose, medium, and high-density soil) on the pile behavior, and the performance of pile-stabilized slopes. The performance of the stabilized slopes was analyzed by evaluating the factor of safety, lateral displacement and bending moment of piles, and critical slip mechanism.

## 2. Methodology

### 2.1 Used software

The finite difference method (FDM) is one of the oldest numerical methods for solving differential equations**.** This method is used for numerical analysis of continuous, continuous with joint, and quasi-continuous environments. $FLAC^{3D}$ is a software based on finite difference method that has the ability to model surface and underground structures in earthen and rock environments such as tunnels, foundations, piles, etc. In addition, this software can consider the effect of the presence of maintenance structures such as anchors, piles, cables, in-situ concreting, etc.

There are conditions for modeling the level of discontinuity or slip level in this software, which is used to model specific discontinuity levels between two or more network segments. In addition, with the help of this software, the behavior after the failure of materials and plastic deformations can be studied. This software has cube-shaped elements, and each one's behavior is based on the behavior characteristics that were set up for it, the behavior model that controls it, the boundary conditions, and the forces that are acting on it (Itasca Consulting Group, 2012).

### 2.2 General process of modelling

In order to simulate the behavior of slopes reinforced with numerical methods, the behavior of materials must be defined correctly (Sarkhani Benemaran and Esmaeili-Falak 2020, Sarkhani Benemaran *et al*. 2022). In accordance with

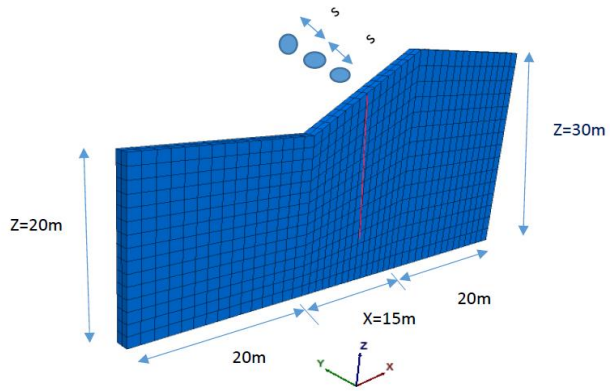


Fig. 1 Geometry of the model made in the present study

reality, and for this purpose, several components must be determined for modeling, which is described below. In all models made in this study, the following trend has been followed:

In all models made in this study, the following trend has been followed:

- Making the initial geometry of the model (2.2.1)
- Assigning appropriate behavioral model and geotechnical characteristics to different parts of the model such as the soil environment around the pile, piles, and interaction layer (2.2.2)
- Applying boundary conditions around the block and the conditions of initial stresses in it (2.2.3)
- Solve the model until the initial equilibrium is reached before making changes in the model (2.2.4)
- Calculation of safety factor by shear strength reduction method (SSRM) (2.2.5)

### *2.2.1 Making the initial geometry of the model*

Due to the symmetry of the problem, only one of the piles is modeled. To achieve reasonable accuracy, around the pile area and the slope surface due to turbulence in the field instead of stress as well as larger displacements at the place of maintenance pressure, the dimensions of the meshes along the longitudinal slope compared to other smaller points were selected, and the distance from the pile to the dimensions of the elements was considered larger (Fig. 1). The soil area was built with brick elements. A non-uniform three-dimensional grid consisting of approximately 45,000 elements was used for networking the models. The displacement boundary conditions in the model are in the order: the ground surface and slope are free to move, the lateral surfaces have hinged boundaries and prevent any movement in the direction perpendicular to these planes, and the model floor is fixed in all directions. The tip of the pile is chosen as a joint. On the upper surface of the block, which represents the ground surface, in the presence of surface loads such as traffic load or building load, this load was applied as a uniform spread load.

### *2.2.2 Assigning appropriate behavioral model and geotechnical characteristics*

#### *2.2.2.1 The soil environment around the pile*

The Mohr-Columb plastic model of behavior was considered a suitable model for soil mass because this model allows the development of plastic areas near the failure surface and leads to more accurate solutions than the complete elastic model.

In the Moher-Columbus behavioral model, three parameters of cohesion, internal friction angle, and dilation angle are used to determine the behavior of the soil. The values related to these parameters are extracted from Table 1 and entered into the models. In $FLAC^{3D}$ software, the bulk modulus, and soil shear modulus are used instead of the deformation modulus and Poisson's ratio. According to the following equations, the bulk and shear modulus of the soil can be calculated according to the modulus of deformation and the Poisson's ratio (Itasca Consulting Group, 2012)

$$K = \frac{E}{3(1\text{-}2\nu)} \quad (1)$$

$$2G = \frac{E}{2(1+\nu)} \quad (2)$$

where, $K, G, E$ *and* $\nu$ present the bulk modulus of soil, the shear modulus of soil, the modulus of deformation, and the Poisson's ratio.

#### *2.2.2.2 Structural piles*

The pile element is used to simulate the behavior of a pile. The pile element offers a combination of beam and cable features. This means that the pile element can simulate a combination of the pile's tensile, shear, and flexural behavior. The pile interacts with the grid through normal and shear coupling springs with nonlinear cohesion and friction. The mechanical properties of the normal (vertical) and shear coupling springs are supplied in Sun *et al.* (2014).

These springs, which attach the pile element to the surrounding soil nodes, act as “slider springs” that transfer force and displacement from the soil to the pile and vice versa. The shear behavior of the pile-grid interface during relative shear displacement between pile and soil is presented numerically through spring shear parameters such as shear stiffness, shear cohesion, shear friction angle, and visible circumference of the pile and soil cross-section. On the other hand, the normal behavior of the pile-grid interface during relative displacement between the pile and the soil through normal spring parameters such as normal stiffness, normal cohesion, and normal friction angle of the environment around the pile and soil cross-section are presented.

### *2.2.3 Applying boundary conditions around the block and the conditions of initial stresses in it*

The boundary conditions of displacement in the model are, a) the ground and slope are free from displacement, b) the lateral surfaces have roller boundaries and prevent any movement in the direction perpendicular to these planes, and c) the model floor is fixed in all directions. On the top plate of the block, which represents the ground level, in the presence of surface loads such as traffic loads or loads of buildings, this load is applied as a uniform wide load. Fig. 2

Table 1 The properties of used materials

| Parameter | Unit | Dense sand | Average dense sand | Loose sand | Concrete pile |
|---|---|---|---|---|---|
| Density | $kN/m^3$ | 1750 | 1700 | 1650 | 2300 |
| Elasticity modulus | $MPa$ | 60 | 40 | 20 | 25000 |
| Poisson's ratio | – | 0.3 | 0.3 | 0.3 | 0.2 |
| Friction angle | ° | 40 | 35 | 30 | – |
| Dilation angle | ° | 10 | 5 | 0 | – |
| Cohesion | $kPa$ | 10 | 10 | 10 | – |

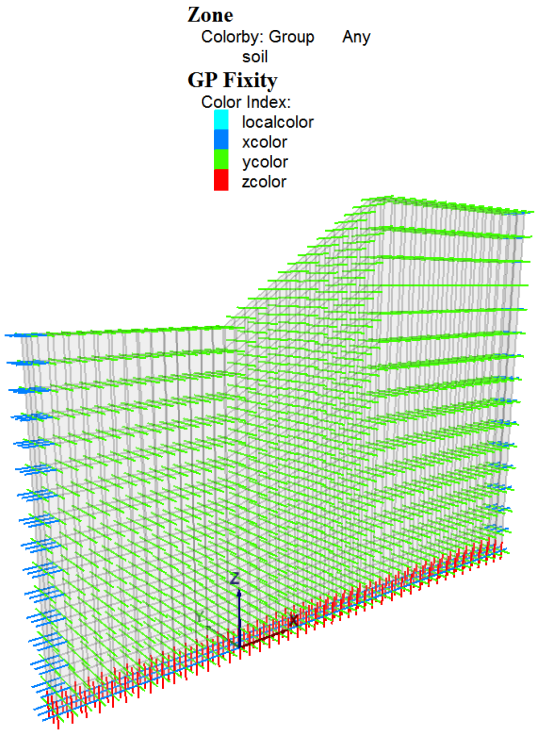


Fig. 2 Limiting the lateral planes of the model against displacement along the x, y and z directions

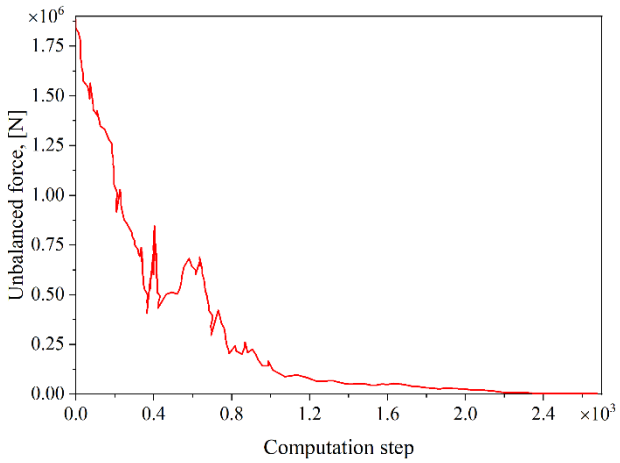


Fig. 3 Displacement along the x, y and z directions The state of unbalanced forces in the model

shows how the boundary conditions are applied to the models.

It is assumed that the distribution of initial stresses is according to Eq. (3).

$$\sigma_h = k_0 \sigma_v \tag{3}$$

where $\sigma_v = \gamma z$ is the vertical stress, $\sigma_h$ is the horizontal stress and $k_0$ is the coefficient of lateral earth pressure at rest mood. It should be noted that the lateral pressure coefficient of the earth in two horizontal directions $(x \; and \; y)$ is considered equal $k_{0x} = k_{0y}$.

#### 2.2.4 Solve the model until the initial equilibrium is reached

The constructed model must be implemented before calculating the $FOS$ with the method of $SSRM$ and achieving the ground equilibrium position according to the given geotechnical properties. After implementing the model, the in-situ stresses are located on the ground, and due to the lack of calculations, the stress field is uniform, and no turbulence is seen in them. It should be noted that the condition for the model to reach equilibrium in $FLAC^{3D}$ software is that the unbalancing forces approach and the velocity of the node point to zero, and the displacements of each node point are fixed.

For example, Fig. 3 shows the state of unbalanced forces in the model until the equilibrium is reached before drilling. Typically, the node displacements are zero after the model reaches equilibrium and before changes are made and the $FOS$ is calculated. This is done to prevent pre-drilling deformation from interfering with the drilling operation. However, the initial stress application stage and the $FOS$ calculation can be combined in calculating the slope $FOS$.

#### 2.2.5 Calculation of $FOS$ by $SSRM$

$FOS$ is often calculated by the ratio of shear strength to the minimum shear strength required to prevent failure. The principal way to calculate the FOS of finite element or various finite element software is to reduce the shear strength to such an extent that failure occurs. The $FOS$ is equal to the ratio of the actual shear strength of the substrate to the reduced strength at the moment of failure. The technique of reducing shear strength in finite element software has been performed to calculate the slope $FOS$ combined with several different materials (Zeinkiewicz *et al.* 1975).

To perform a slope stability analysis with $SSRM$, a set of stability analyses with reduction of shear strength parameter $C^{trial}$ and $\varphi^{trial}$ is defined as Eqs. (4) and (5) (Sun *et al.* 2014).

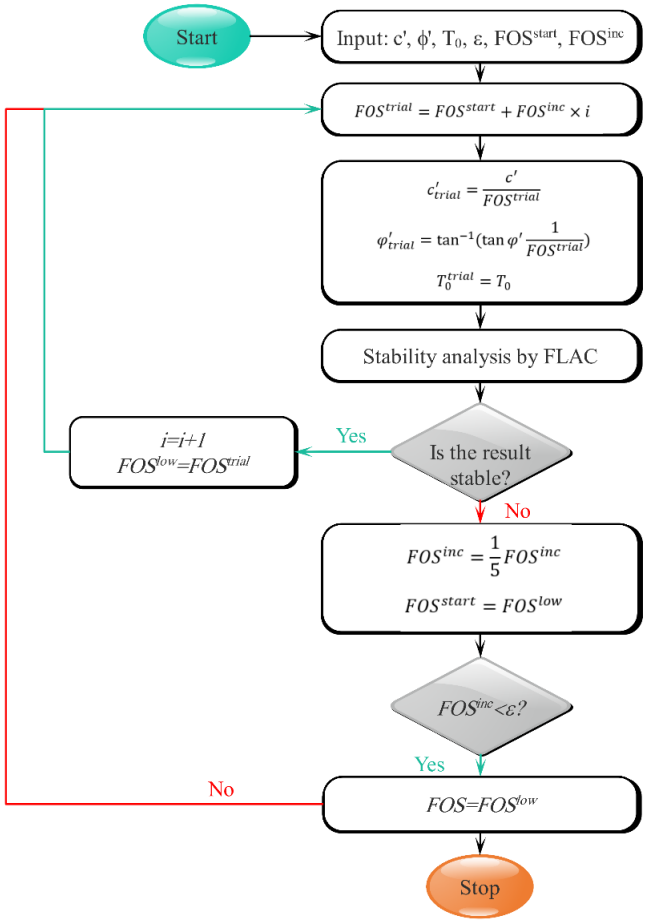


Fig. 4 Analytical model for calculating the FOS of a slope stabilized with pile (Sun *et al*. 2014)

$$c^{trial} = \frac{1}{FOS^{trial}} c \tag{4}$$

$$\varphi^{trial} = \frac{1}{FOS^{trial}} \varphi \tag{5}$$

where $c$ and $\varphi$ are the actual shear strength parameters and $FOS^{trial}$ is the experimental safety factor. Fig. 4 shows the analytical model for calculating the slope $FOS$ reinforced with piles. In Fig. 4, $FOS^{trial}$ will be one to judge the stability of the system. Therefore, the value of $FOS^{trial}$ has been reduced or increased until the slope fails. After a sloping failure, $FOS^{low}$ or $FOS^{high}$ replaces the previous $FOS^{trial}$. A point between the upper and lower limit is tested in the next step. If the simulation converges, the upper interval is replaced. This process is repeated until the difference between the upper and lower intervals is less than the strain determined. In this study, the non-convergence option has been considered a suitable failure indicator.

### 2.3 Validation of the software used

In this section, to validate the results of the software used, different models were created and compared with other numerical codes, which in all cases, the results of the comparisons were favorable. In order to ensure the correct execution of the analyzes, three validation cases have been performed to check the stability of the reinforced slope without piles to check the stable slope at different $S/D$ and in different positions of the piles. For this purpose, the analyzes performed in several studies have been simulated, and their results are as follows.

#### 2.3.1 First verification: FOS of non-stabilized slope (Dai et al. 2017)

Dai *et al.* (2017) using *ABAQUS* finite element software, investigated the stability of unreinforced soil slope by two methods of *SSRM* and displacement of the characteristic point in two dimensions. The geometry of the problem under consideration is as shown in Fig. 5.

Fig. 6 shows a comparison of $FLAC^{3D}$ and *ABAQUS* software for different cohesion of 5, 10, 15, 20, 25, 30, 35 kPa and a friction angle of 20. As can be seen from the figure, with increasing cohesion, the FOS has raised. Also, the numerical results obtained from $FLAC^{3D}$ software is in good agreement with the numerical values of *ABAQUS* software. For further study in Fig. 6, the $FOS$ changes in terms of friction angle of 10, 15, 20, 25, 30, 35 degrees and assuming a constant cohesion of 15 kPa are presented. As

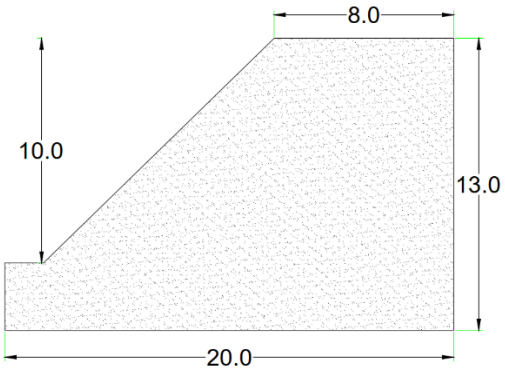


Fig. 5 The geometry of the model made in the first validation (units per meter)

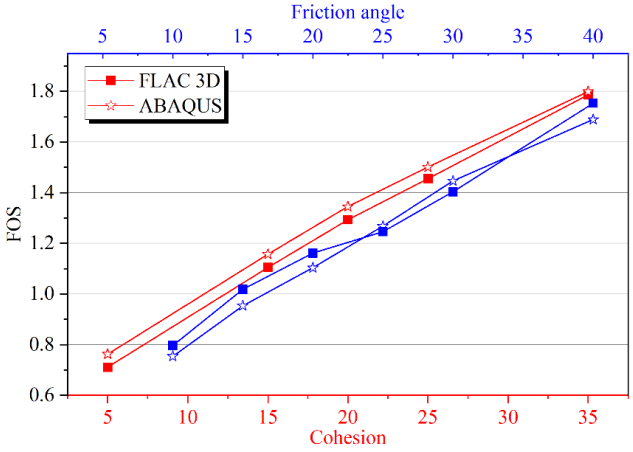


Fig. 6 Changes in $FOS$ with soil cohesion and friction angle in the present modeling and Dai *et al.* (2017)

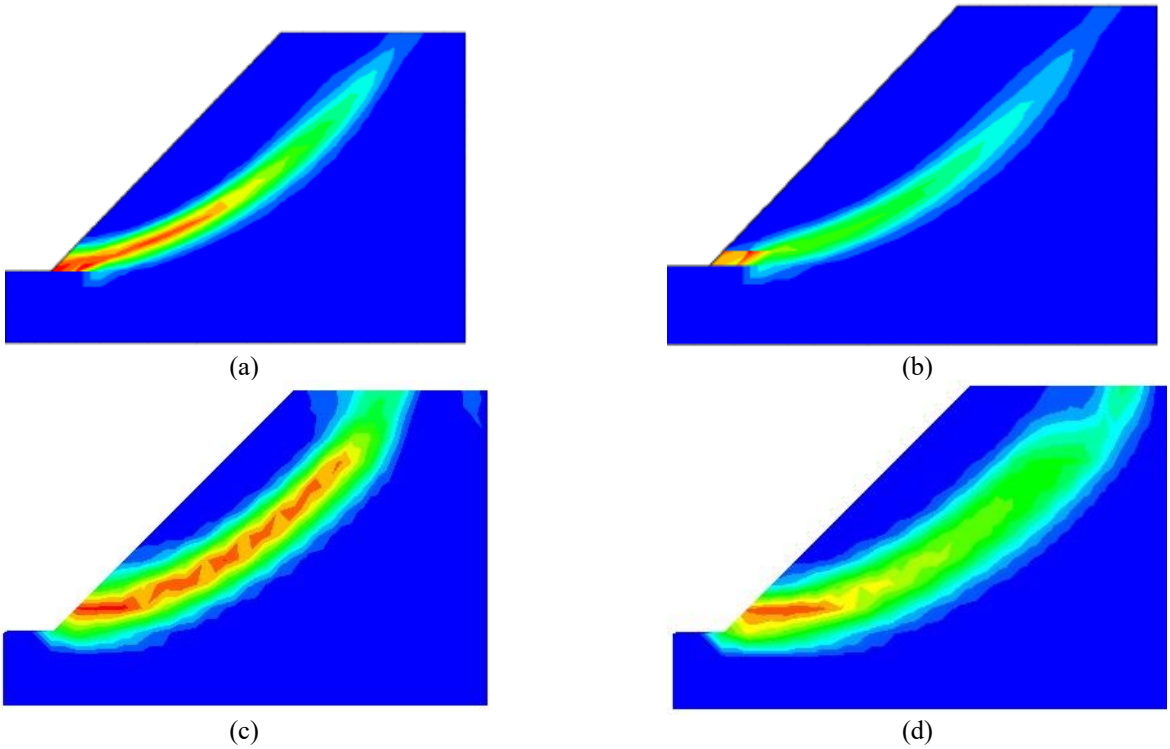


Fig. 7 The failure surface in terms of shear strain rate changes in the two software: (a) and (b) c=15 kPa and 25 kPa in $ABAQUS$, (c) and (d) c=15 kPa and 25 kPa in $FLAC^{3D}$

expected, the $FOS$ has increased similarly in $FEM$ and $FDM$ methods with raising friction angle**.** According to the results of the validations performed, the performance of the $FLAC^{3D}$ can be adequately understood. Also, Fig. 7 present the failure surface in terms of shear strain rate changes in the two software.

### *2.3.2 Second verification: FOS of stabilized slope (Shooshpasha and Amirdehi 2015)*

Shooshpasha and Amirdehi (Shooshpasha and Amirdehi 2015), by considering the geometric characteristics of the soil slope according to Fig. 1 and in 3D mode and with the help of $ABAQUS$ software to analyze the stability of the slope stabilized with a row of piles and free pile heads by $SSRM$. In this study, $L$, the position of the pile ($X_p/X$) and $S/D$ ratio on the slope performance have been investigated**.** In the analysis, the behavior of elastoplastic materials was based on the Mohr-Columb failure criterion, and the behavior of elastic concrete piles was linear. It should be noted that volumetric elements were used to model the pile, while in this study, elements of pile structures were used. The pile was also placed in the middle of the slope**.**

### *2.3.3 Investigation of the effect of S/D on FOS*

Fig. 8 compares the results of the $FLAC^{3D}$ and $ABAQUS$ software in determining the slope $FOS$ in terms of $S/D$ in a

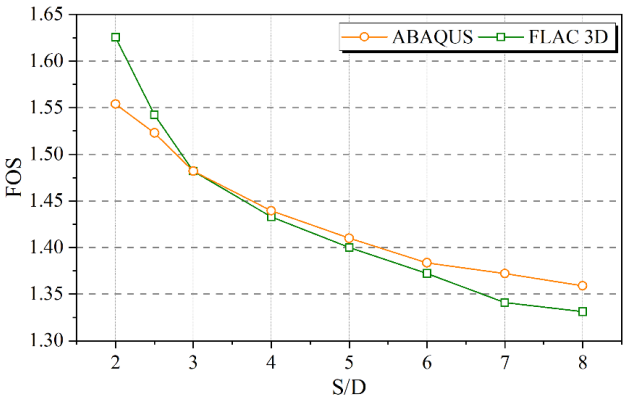


Fig. 8 FOS changes with S/D in the present study and Shooshpas and Amirdehi (Shooshpasha and Amirdehi 2015)

row. As can be seen from this figure, the FOS has decreased with increasing the $S/D$. However, as $S/D$ gets higher further, the FOS gradually declines. In fact, the slope $FOS$ for different piles $S/D$ is close to each other for short piles. It is also clear from this figure that the numerical results obtained from the $FLAC^{3D}$ software is in good agreement with the numerical values of the $ABAQUS$ software. Therefore, according to the obtained results, it is possible to understand the performance of the finite difference method correctly $FLAC^{3D}$ program.

#### *2.3.4 Investigation of the effect of $X_p/X$ on FOS*

This paper investigates the effect of optimal pile position on slope performance with $ABAQUS$ software and $SSRM$. In fact, $X_p$ plays an essential role in the stability of the slope. $X_p$ is the horizontal distance of the pile from the toe of the slope, and $X$ is the horizontal length of the entire slope. $X_p/X = 0$ means that the pile is on the toe of the slope and $X_p/X = 1$ means that the pile is on the crest of the slope. Fig. 9 shows the relationship between the FOS and the optimal $X_p/X$ ratio for comparing the $FLAC^{3D}$ and $ABAQUS$ software in determining the optimal position of the pile at $S = D$. It should be noted that the initial length of the pile used to determine the optimal position in $FLAC^{3D}$ software is 18 meters. As can be seen from the figure, in the present study, the exact optimal position of the pile is about 0.6 above the toe of the slope, with a $FOS$ of 1.74.

In this figure, the percentage of error is also presented. It is also clear from this figure that the numerical results obtained from the $FLAC^{3D}$software are in good agreement with the numerical values of the $ABAQUS$ software. Therefore, according to the obtained results, it is possible to understand the performance of the finite difference method of correctly $FLAC^{3D}$ program.

### *2.4 Modelling*

In this section, using 3D modeling, the stability of pile-reinforced slopes by $SSRM$ is investigated by $FLAC^{3D}$ finite difference software**.** The effect of pile length ($L$) (8, 10, 12, 14, 16, and 18 m), different pile distances from each other ($S/D$=2, 3, 4, and 6), pile head condition (free and fixed head) and sand compaction (loose, average dense, and dense sand) effect on pile lateral displacement, slope $FOS$ and pile behavior in three soil types have been investigated.

In the analysis, the behavior of elastoplastic materials is based on the Mohr-Columb failure criterion, and the behavior of elastic concrete piles is linear. The concrete pile used has a diameter of 0.8 meters. The geometry of the slope and the dimensions of the numerical model used are in accordance with Fig. 1. The specifications of used materials for modeling are given in Table 1.

## 3. Results and discussions

### *3.1 Investigation of the effect of $L$ on $FOS$ of slope*

In this section, the effect of $L$ on the $FOS$ of slope for three types of high density, medium dense, and loose dense sandy soils have been investigated**.** As shown in Fig. 10, with increasing $L$, the $FOS$ has risen in all three soil types. However, when $L$ exceeds the critical length ($L_{cr}$), the $FOS$ tends to be a constant value, and the depth of the slip surface does not change. The $L_{cr}$ of the pile is $L$ after which the increment in $L$ over the slope $FOS$ is negligible, and the FOS is fixed at that length.

According to Fig. 10, it can be seen that for $L$ at 20 meters, the $FOS$ has been fixed, and based on the explanations mentioned above, this length is considered as the $L_{cr}$ at $S = 2D$ mode in medium density sandy soils. In dense sandy soils, according to Fig. 10, from 18 m length onwards, the trend of increasing $FOS$ has been fixed by increasing the $L$, indicates that this length is considered as the $L_{cr}$ at $S = 2D$ in dense sandy soils. In loose sandy soils, according to Fig. 10, from 20 m length onwards, the upward trend of FOS has been fixed by increasing the $L$, and this indicates that this length is $L_{cr}$ in loose sandy soils. The $L_{cr}$, which gives the highest $FOS$, varies at different $S/D$ ratios. By reducing the $S/D$ ratio, due to the function of the wall such as piles, the integrity, and cohesion of the soil and piles have enlarged; Therefore, the lateral bearing capacity of the reinforced slope is considerably got higher and the affected surface due to $L_{cr}$ is enlarged; In other words, $L_{cr}$ declines with increasing distance between the piles.

Soil properties have a significant effect on $L_{cr}$. The effect of soil density on $FOS$ and slope performance for all three types of high, medium, and loose density soil for various $S/D$ has been investigated. As can be seen from Fig. 10, dense sandy soils have a higher $L_{cr}$, it means a higher $FOS$ than medium-density and loose sandy soils; In other words, with increasing soil density, the $FOS$ has got bigger.

The $L_{cr}$, which gives the highest $FOS$, varies at different distances of the pile. The $S/D$ ratio has a significant impact on $L_{cr}$; That is, by increasing the $S/D$ ratio, $L_{cr}$ in all three types of soil, is reduced. The shorter the $S/D$ ratio, the greater the integrity and cohesion of the soil and piles due to the wall function of the piles. On the other hand, this study will have more FOS than these results are shown in Fig. 11. This is because as the $S/D$ ratio increases, the lateral bearing capacity of the reinforced slope has greatly

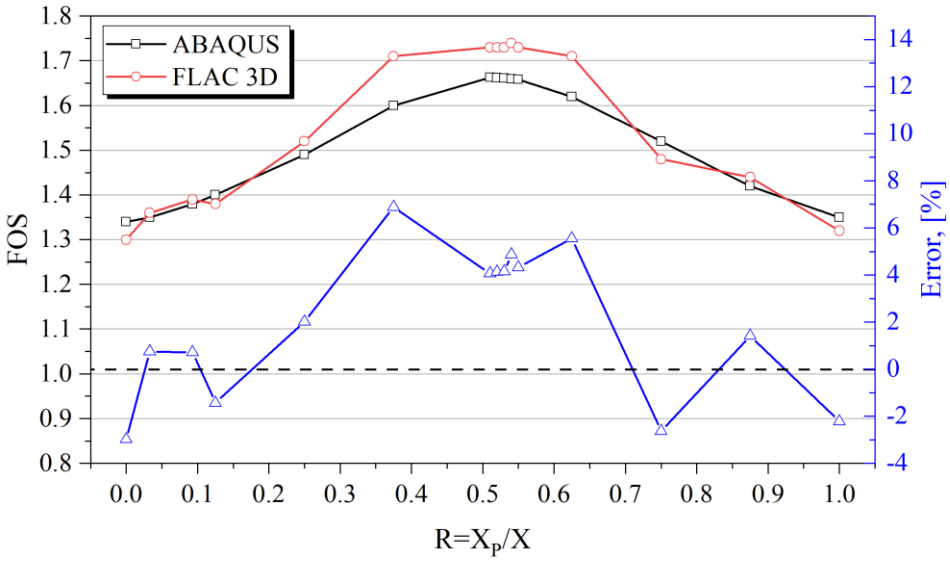


Fig. 9 Diagram of $FOS$ values according to different positions of piles on the slope in the present study and Shooshpasha and Amirdehi (Shooshpasha and Amirdehi 2015)

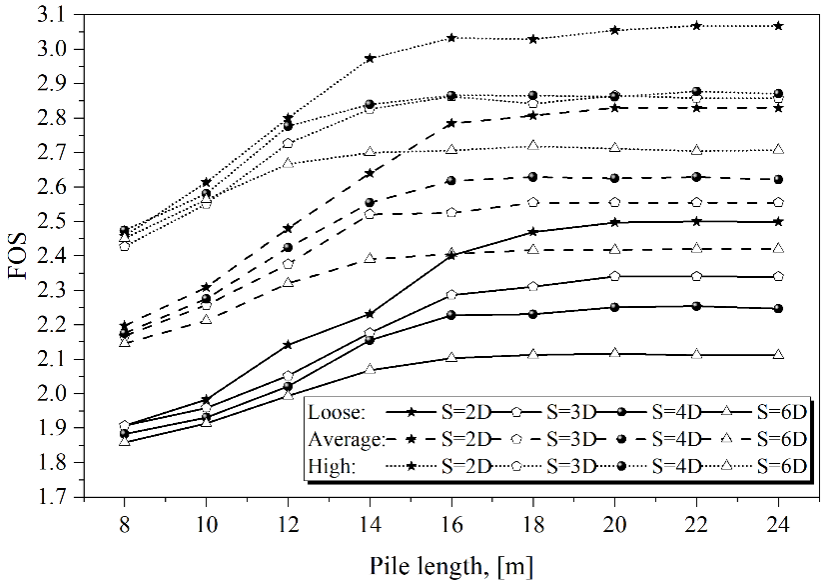


Fig. 10 Comparison diagram of the effect of $L$ on $FOS$ for loose density sand, average density sand, and high-density sand

surged, and the affected surface due to $L_{cr}$ is enlarged; In other words, the $L_{cr}$ declines with increasing $S/D$ ratio. Fig. 11 shows the exact $L_{cr}$ at several $S/D$ ratios for three types of soil with different densities. As can be seen from the figure, $L_{cr}$ goes down with raising the $S/D$ ratio.

To investigate the effect of $S/D$ of piles, four analyzes were performed for each soil type with $S/D$ at 2, 3, 4, and 6. In order to further study the effect of the S/D of the piles on the FOS, the figure of the maximum values of the $FOS$ against the $S/D$ ratio is drawn in Fig. 11. As can be seen from the figure, the FOS decreases rapidly initially as the $S/D$ increases, but as the $S/D$ ratio between the piles goes up further, the $FOS$ gradually declines. It is also observed that for short piles, the FOS of the pile reinforced slopes at different $S/D$ is close to each other, but with increasing the

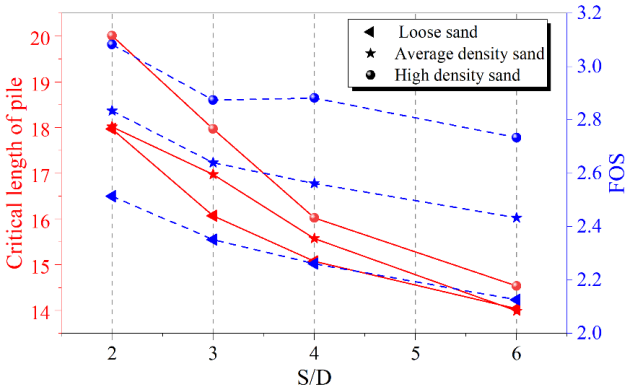


Fig. 11 Comparison of the effect of S/D on $L_{cr}$ and FOS of slope

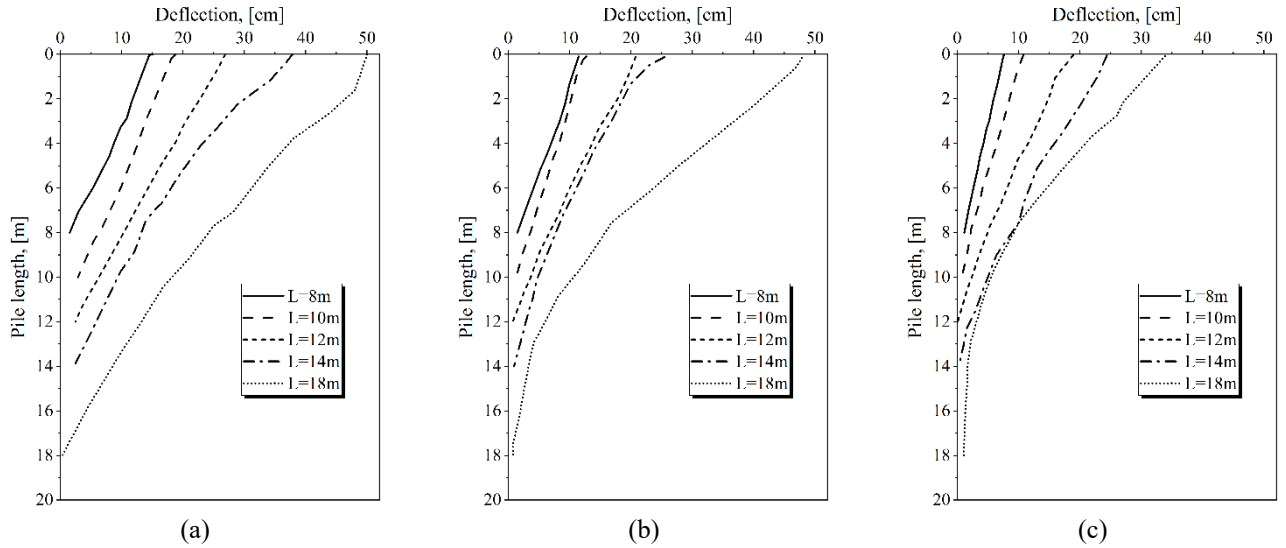


Fig. 12 Comparison of lateral displacement along pile length versus pile length change in: (a) Loose sandy soil, (b) Average density sand, and (c) High density

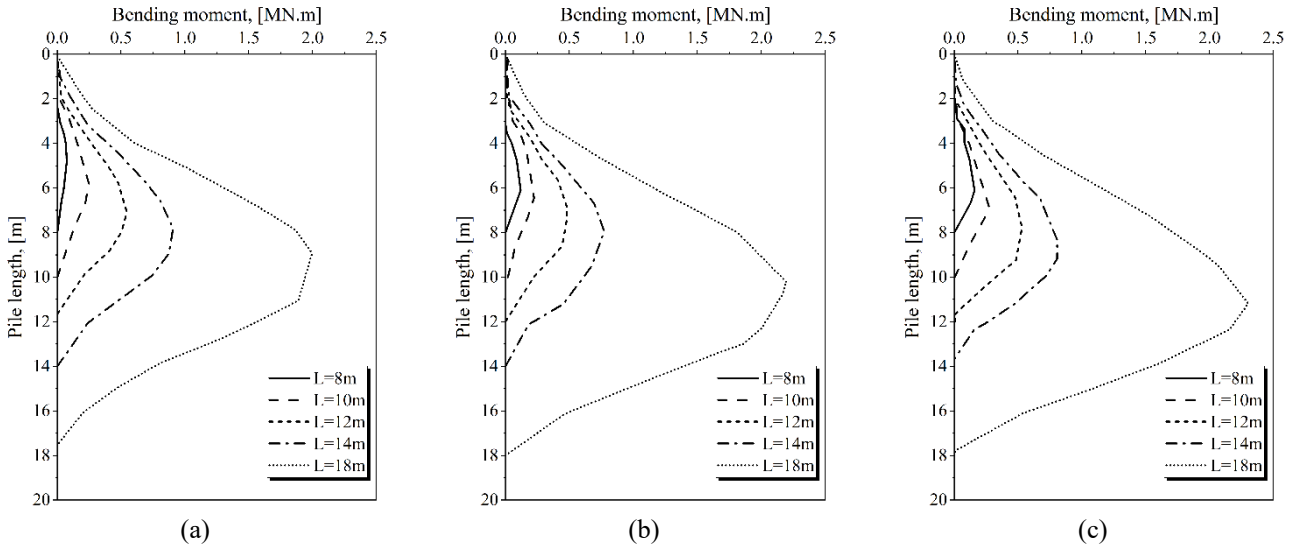


Fig. 13 Comparison of the bending moment along pile length versus pile length change in: (a) Loose sandy soil, (b) Average density sand, and (c) High density

$L$ at different distances, the difference between the $FOS$ increases; Therefore, with increasing the $S/D$ ratio, the $FOS$ has decreased.

### *3.2 results of modeling on the behavior of free head piles*

#### *3.2.1 Effect of increasing the $L$ in lateral displacement*

Figs. 12(a)-12(c) show lateral displacement in piles with different lengths $(L)$ for $S = 2D$ and $D = 0.8\,m$ in three types of loose, average density, and high-density sandy soil. As can be seen, with increasing the depth of the piles, the amount of lateral displacement due to the effects of enclosing stress is reduced; On the other hand, at the top of the pile, due to its proximity to the ground, there will be more freedom of movement and consequently more lateral displacement than at lower depths. The higher $L$, the more lateral displacement of the piles. When $L$ exceeds its $L_{cr}$, the displacement value reaches a uniform distribution, but when $L$ is less than its $L_{cr}$, the deformation gets higher mainly linearly with depth. The reason for this linear behavior is the supply of slip-resistant force at the end of the pile and the presence of increased pressure on the top of the pile before $L_{cr}$.

#### *3.2.2 Effect of increasing $L$ in bending moment*

In Figs. 13(a)-13(c), the comparison of bending moment in piles with D=0.8 m and with different $L$ in three types of soils with different densities is shown. As shown in the figure, the bending moment is zero at the top and end of the pile due to the freedom of movement. As shown in the figure, the amount of bending moment raises with increasing $L$. This is because by increasing $L$ until it is less than $L_{cr}$, the slip surface gets bigger, and the pile covers a

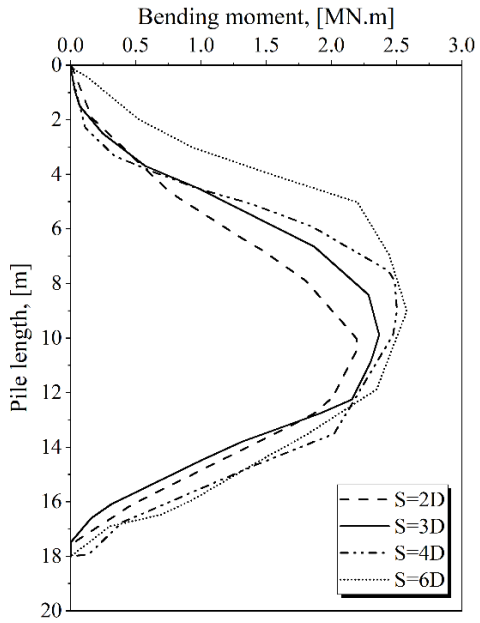


Fig. 14 Comparison of bending moment in piles with different $S/D$ ratio in medium density sandy soils

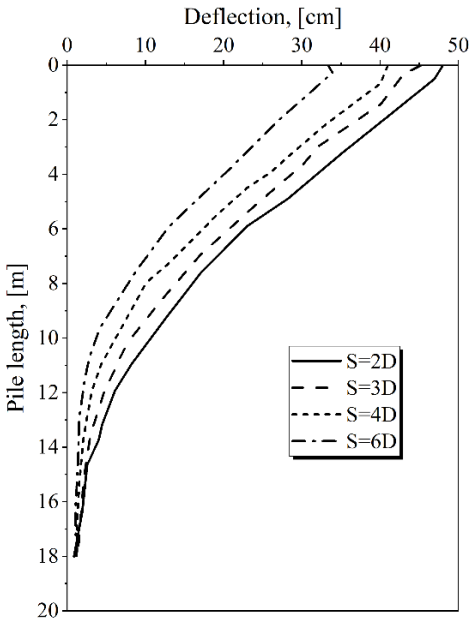


Fig. 15 Comparison of lateral displacement in piles with different $S/D$ ratio in medium density sandy soils

larger part of the failure mass and is more resistant to sliding, resulting in more force and moment in a pile. On the other hand, the position of the maximum bending moment tends towards the lower half of the pile, and the moment depth is reduced. As long as $L$ exceeds its $L_{cr}$ and the maximum bending moment is reached to a uniform distribution. On the other hand, the maximum bending moment from 0.06 MN.m in an 8-meter pile to 2 MN.m in an 18-meter pile has increased. As a result, an increment of approximately 30 times in maximum bending moment is achieved by 2.25 times the length of the used piles. According to the diagrams shown, it can be concluded that with more compacting soil, the maximum bending moment has decreased**.**

### *3.2.3 The effect of the distance of the piles on the bending moment and lateral displacement of the pile*

The effect of different $S/D$ of piles on bending moment in medium density sandy soil has been investigated. As can be seen from Fig. 14, as the $S/D$ ratio increases, the bending moment in a pile rises, and the position of the maximum bending moment goes up and is located in the upper half of the pile. In other words, as the $S/D$ ratio increases, the maximum amount of bending moment surges, and its depth cuts down. This is because the load area of each pile, which is affected by the lateral displacement of the soil, has expanded with increasing $S/D$.

Fig. 15 shows a comparison of the effect of different $S/D$ on the lateral displacement of piles in medium-density sandy soils. As can be seen, the larger the $S/D$ ratio, the more lateral displacement of the piles. This is because as the $S/D$ ratio decreases, the behavior of the piles becomes more like that of the continuous network, and the effect of arching of the soil becomes more apparent. The lateral bearing capacity of the pile is reduced by decreasing the bearing capacity of the pile, which causes the phenomenon of arching. Also, because $L_{cr}$ has declined by raising $S/D$, and because $L_{cr}$ for medium-density sandy soil at $S = 2D$ is greater, the lateral displacement of the pile is greater than other $S/D$ ratios.

### *3.2.4 Effect of soil density on lateral displacement and bending moment of the pile*

Fig. 16 shows the lateral displacement for the $L$ of 12 m in three different soil types. As can be seen from the figure, loose sandy soils have the highest amount of lateral displacement, and dense sandy soils have the least amount of lateral displacement. In other words, with increasing soil density, the lateral displacement in a pile is reduced, and the lateral displacement depth in dense sandy soils is less than in medium and loose sandy soils. In other words, with more compacting soil, the relative hardness of soil and pile has increased, which makes the pile behavior in dense soil as elastic, and also in dense sandy soil due to locking between soil, grains cannot easily move sandy soil with medium density and loose, and the lateral bearing capacity of the pile has been increased. That is, the lateral bearing capacity of the pile in dense sandy soils is higher than in loose sandy soils, and the lateral displacement in a pile is reduced. Due to the reduction in lateral resistance of soil to piles and increase in shear strength in soil and also because with increasing soil density, soil hardness and strength rise and the slope becomes more stable and soil grains cannot move easily in medium and loose sand soil, the lateral displacement of the pile is lowered as a result.

Fig. 17 shows a comparison of bending moments for $L$ of 18 m in three types of sandy soils with different densities. As can be seen from the figure, loose sandy soils have the highest amount of bending moment, and dense sandy soils have the least number of moments. The maximum amount of bending moment happened in dense soil because with increasing soil density, the lateral bearing

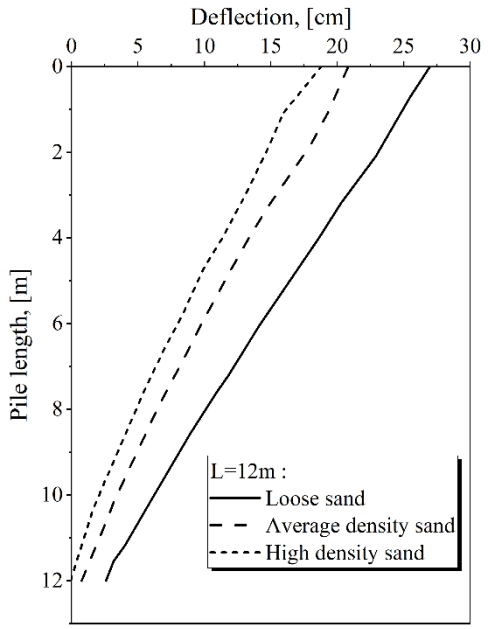


Fig. 16 Comparison of the effect of soil density on lateral pile displacement

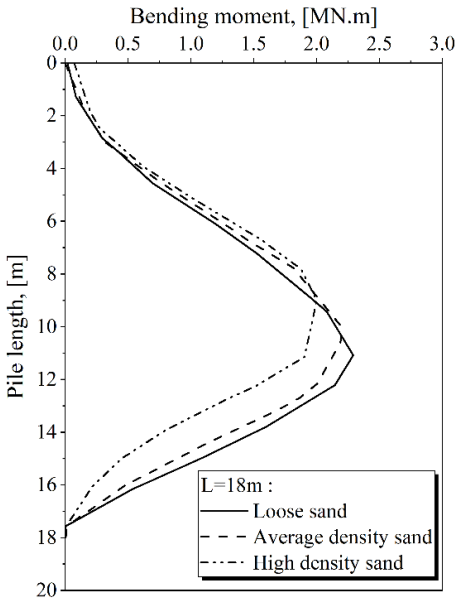


Fig. 17 Comparison of the effect of soil density on bending moment

capacity of the pile has increased, and the maximum bending moment has gone down. Also, due to the fact that with increasing soil density, soil hardness and strength surges and soil slope becomes more stable, and soil grains cannot move easily; as a result, a less bending moment is applied to the pile.

### *3.2.5 Potential sliding surface by the maximum shear strain increment*

#### *3.2.5.1 For different L*

As $L$ increases, the slope FOS become bigger in all three types of dense, medium and loose sandy soils, but when $L$ exceeds its $L_{cr}$, the $FOS$ remains almost constant. As can be seen from the shear strain contours in medium-density sandy soils, with increasing $L$, the slip surface becomes deeper, and the slope $FOS$ increases, but when $L$ exceeds $L_{cr}$, due to the presence of anti-slip forces at the end of the pile, which is in the stable layer, the depth of the slip surface does not increase, and the FOS remains constant (Fig. 18).

#### *3.2.5.2 For different S/D ratio*

The $L_{cr}$, which gives the maximum $FOS$, varies for different pile $S/D$ ratio (Fig. 19). By reducing the distance between the piles, the pile acts much like a continuous pile wall, increasing the integrity and coherence between the soil and the pile. Therefore, the lateral bearing capacity of the pile is getting larger, and the affected surface due to $L_{cr}$ is expanded. In other words, the higher the $S/D$ ratio, the small $L_{cr}$ in all three types of soil, and as the amount of soil density increases, $L_{cr}$ surges. For example, $L_{cr}$ in $S/D = 3$ is 18 meters for dense sandy soils, 17 meters for medium sandy soils, and 16 meters for loose sandy soils. In general, with increasing $L_{cr}$, the $FOS$ has increased, and the maximum values of the $FOS$ have raised with reducing the $S/D$ ratio. As can be seen from the contours, $L_{cr}$ decreases with increasing $S/D$ ratio in medium density sandy soil.

### *3.3 Results of modeling on the behavior of fixed head piles*

#### *3.3.1 Effect of L on the lateral displacement of piles*

Figs. 20(a)-20(c) show lateral displacement in piles in fixed pile head condition with different lengths and in $S = 2D$ and $D = 0.8\,m$ in three types of loose, medium, and dense sandy soils. As can be seen, throughout $L$, the deflection has first increased and then declined to zero. In fact, the lateral displacement of the pile head is almost zero for all $L$ due to the lack of freedom of movement. In fact, increasing $L$ does not affect the displacement of the pile head; however, the piles have a little lateral displacement at the beginning of the depth.

#### *3.3.2 Effect of L on bending moment of piles*

Figs. 21(a)-21(c) show a comparison of a bending moment in a pile with a fixed pile head of $D = 0.8m$ and different lengths. As can be seen in the figures, increasing $L$ has minimal effect on increasing the bending moment. In other words, the bending moment changes with raising $L$ slightly. On the other hand, the maximum bending moment has been changed from 1.16 MN.m in an 8-meter pile to 1.40 MN.m in an 18-meter pile, and as a result, a minimal 1.2-fold increment in the maximum bending moment is achieved by doubling the length of the piles used.

#### *3.3.3 Effect of soil density on lateral displacement and bending moment of piles*

Fig. 22 shows the lateral displacement for $L$ of 14 m in three different soil types under fixed pile head conditions. As can be seen, loose sandy soils have the highest amount of lateral displacement at the beginning of the pile, and dense sandy soils have the least amount of lateral

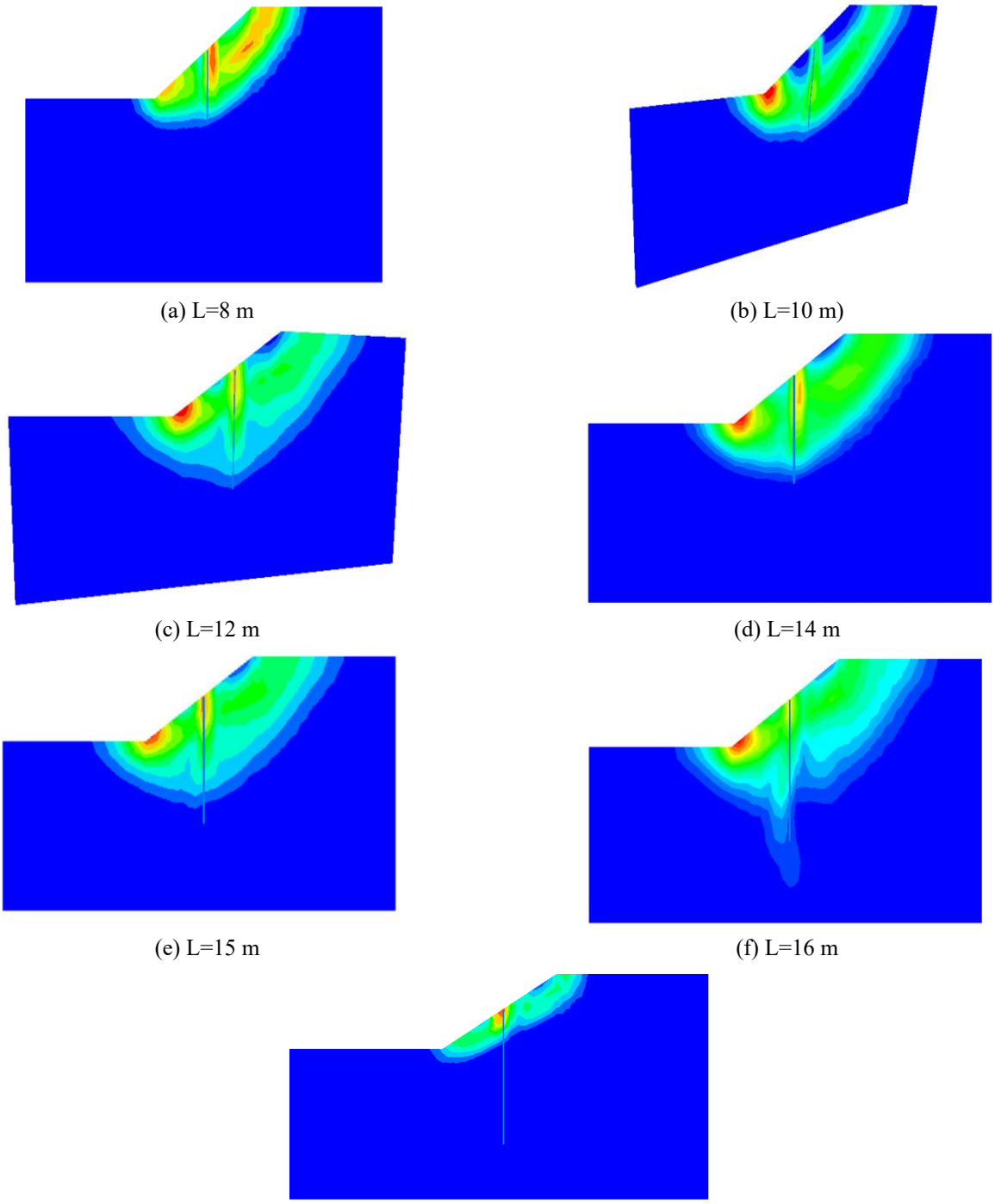

(a) L=8 m (b) L=10 m)

(c) L=12 m (d) L=14 m

(e) L=15 m (f) L=16 m

(g, L=18 m)

Fig. 18 Critical slip level in medium density sandy soil at $S = 2D$ for different $L$

displacement; That is, with increasing soil density, the lateral displacement at the beginning of the pile decreases and gradually increases to zero with increasing pile depth.

Fig. 23 shows a bending moment for $L$ of 14 m in three different soil types under fixed pile head conditions. As can be seen, loose sandy soils have the highest amount of bending moment, and dense sandy soils have less bending moment due to higher shear strength. In other words, it can be said that as the soil density increases, the bending moment decreases.

### *3.4 Effect of pile head condition (fixed or free)*

#### *3.4.1 Pile head condition on the lateral displacement of piles*

Figs. 24(a)-24(c) show a comparison of lateral displacement in the free and fixed pile head condition for a $L$ of 14 m. As can be seen, in the free pile head condition, in all three types of dense, medium, and loose sandy soils, the amount of lateral displacement gradually increases with increasing pile depth, and the maximum

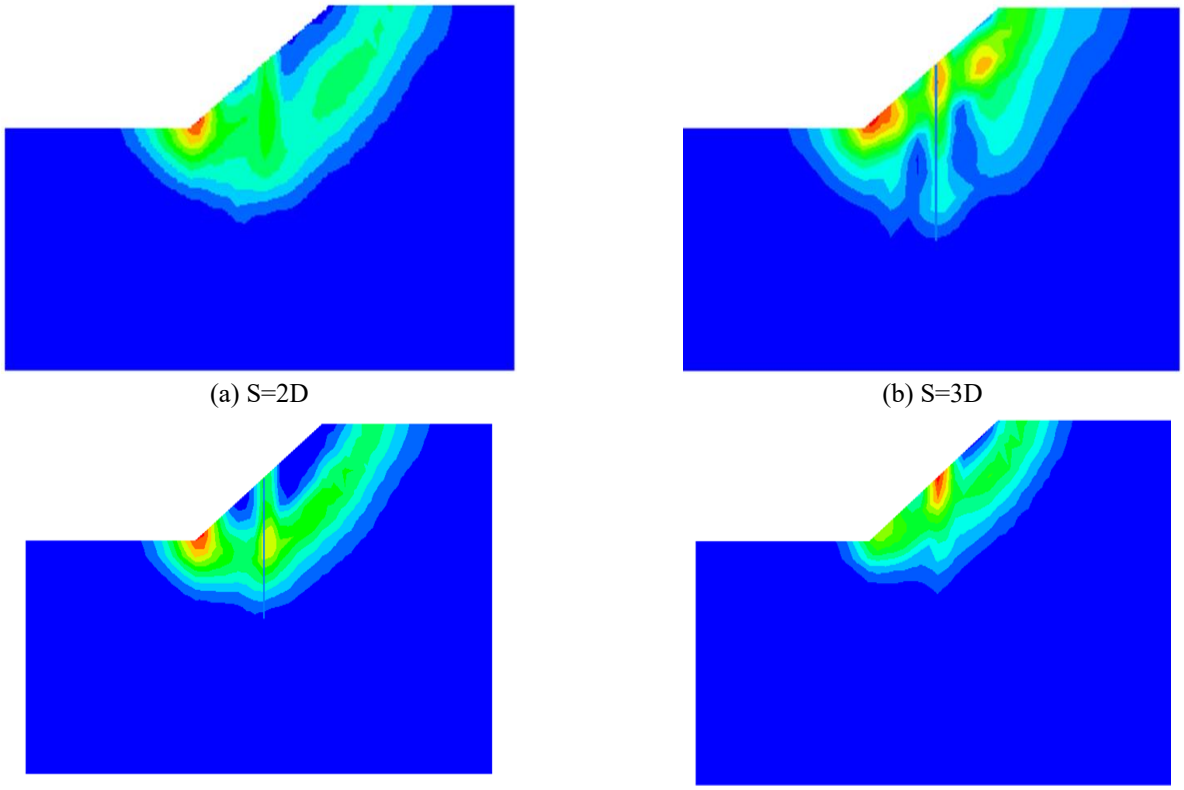

(a) S=2D (b) S=3D

(c) S=4D (d) S=4D

Fig. 19 Critical slip level in medium density sandy soil for different $S/D$ ratio

lateral displacement is formed due to more freedom of movement at the pile head; However, in the case of a fixed pile head, the pile has a small displacement at the beginning of the depth, which gradually decreases to zero as the depth of the pile increases due to lack of freedom of movement.

### *3.4.2 Pile head condition on bending moment of piles*

Figs. 25(a)-25(c) compare the bending moment in the free and fixed pile head condition for $L$ of 14 m. As can be seen, the amount of bending moment at the head and bottom of the free pile head is equal to zero. The amount of moment gradually increases with increasing the depth of the pile, and the maximum amount of flexural anchor is formed on top of the pile. The degree of curvature of the pile is approximately in the middle of the pile, while the pile head is free, but for the fixed pile head, the maximum amount of curvature of the pile is formed on the pile head. In all three types of dense, medium, and loose sandy soils, the maximum amount of bending moment of the free head pile is formed approximately in the center of the pile, but when the pile is fixed, the amount of moment gradually increases with increasing pile depth and the maximum amount of bending moment is formed above the pile. The greater the amount of bending moment at the shallow depths of the pile in the fixed pile head condition indicates the effect of the inertial force due to the structure on the pile performance.

As can be seen, in all three types of dense, medium, and loose sandy soils, the amount of curvature of the pile is almost in the middle of the pile, while the pile head is free, but for a fixed pile head, the highest amount of pile curvature is formed on the pile head.

## 4. Conclusions

In this study, the performance of earth slope reinforced with piles and the behavior of piles under static load, by shear reduction strength method and by the finite difference software ($FLAC^{3D}$) has been investigated. Parametric studies were conducted to investigate the role of pile length ($L$), different pile distances from each other ($S/D$), pile head conditions, the effect of sand density on pile behavior, and the performance of pile-stabilized slopes. The results of the analysis were presented as follows:

- As the $L$ increases, the slope factor of safety ($FOS$) increases in all three types of dense, medium and loose sandy soils, but when the $L$ exceeds its critical length ($L_{cr}$), the $FOS$ remains almost constant. As seen from the shear strain counters in medium density sandy soils, with increasing $L$, the slip surface becomes deeper, and the slope $FOS$ increases. However, when the $L$ exceeds $L_{cr}$, due to the presence of anti-slip forces at the end of the pile, which is located in the stable layer, the depth of the slip surface does not increase, and the $FOS$ remains constant.
- The $L_{cr}$, which gives the maximum $FOS$, is different for different $S/D$ ratios. By reducing the $S/D$ ratio, the pile acts very much like a continuous pile wall, increasing the integrity and coherence between the soil and the pile, and

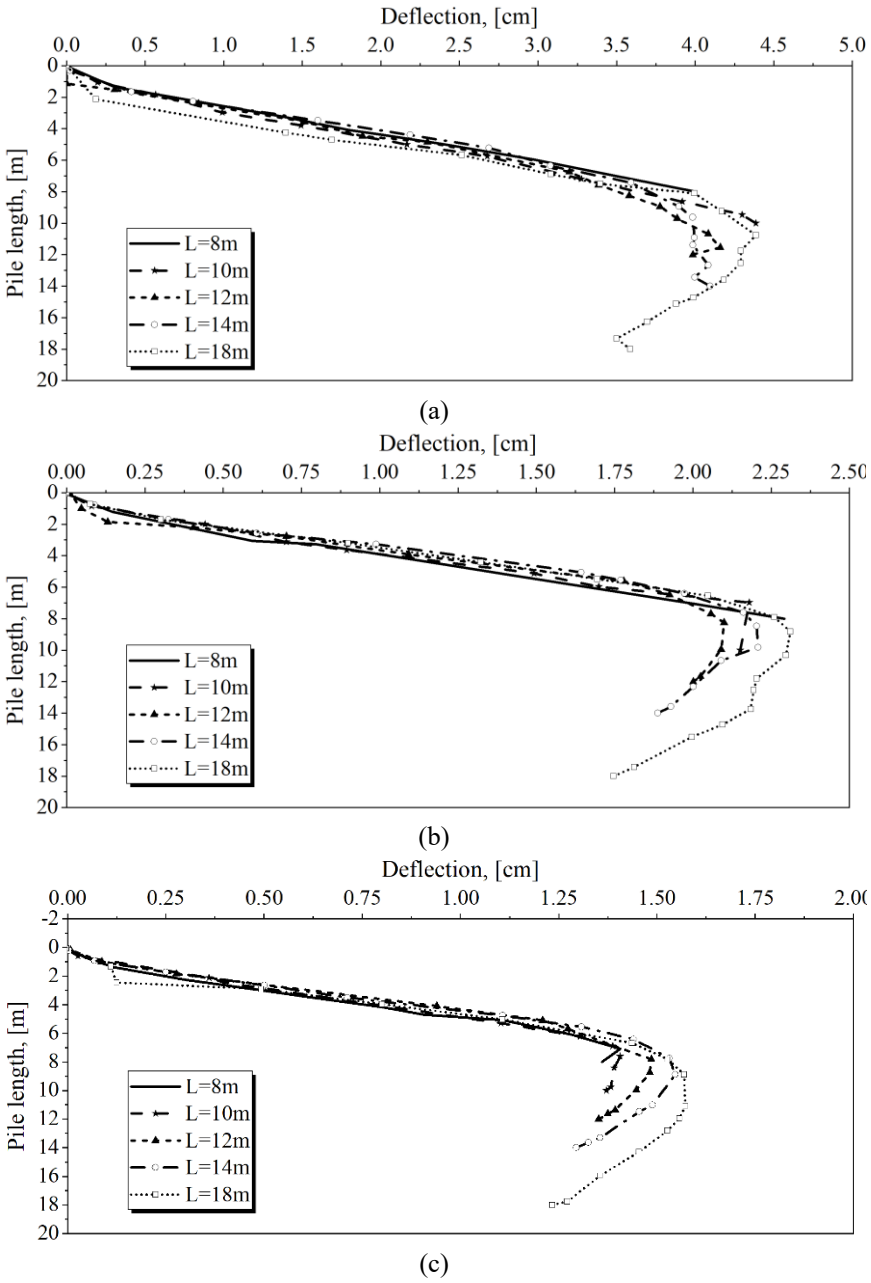


Fig. 20 Comparison of lateral displacement along pile with change in pile length in: (a) loose, (b) medium density, and (c) high density sandy soil at fixed pile head

the effect of the arching phenomenon becomes more visible; Therefore, the lateral bearing capacity of the pile is increased and the affected surface due to $L_{cr}$ is expanded. In other words, with increasing $S/D$ ratio, $L_{cr}$ in all three types of soil has decreased and as the density of the soil increases, $L_{cr}$ increases. In general, with increasing $L_{cr}$, the $FOS$ has increased, and the maximum values of the $FOS$ have increased with decreasing $S/D$ ratio. $L_{cr}$ for dense sandy soils is less than $L_{cr}$ for medium and loose sandy soils.

• With increasing $L$, the amount of lateral displacement has decreased due to the effects of confinement stress; On the other hand, at the top of the pile, due to its proximity to the ground, there will be more freedom of movement and consequently more lateral displacement than at lower depths. Also, with increasing $L$ from each other, the lateral displacement of the pile head increases. When the $L$ exceeds its $L_{cr}$, the pile displacement changes reach a uniform distribution, but when $L$ is less than $L_{cr}$, the lateral displacement depth increased. This linear behavior is due to less slip-resistant forces at the end of the pile and increased pressure on the pile.

• As $L$ increases, the amount of bending moment in the piles increases, and the position of the maximum bending moment moves downwards and is formed in the lower half of the pile and the depth of the moment decreases. This is because by increasing $L$, as long as $L$ is less than $L_{cr}$, the slip surface increases, and the pile covers a larger part of the sliding mass and is more resistant to slipping, resulting in

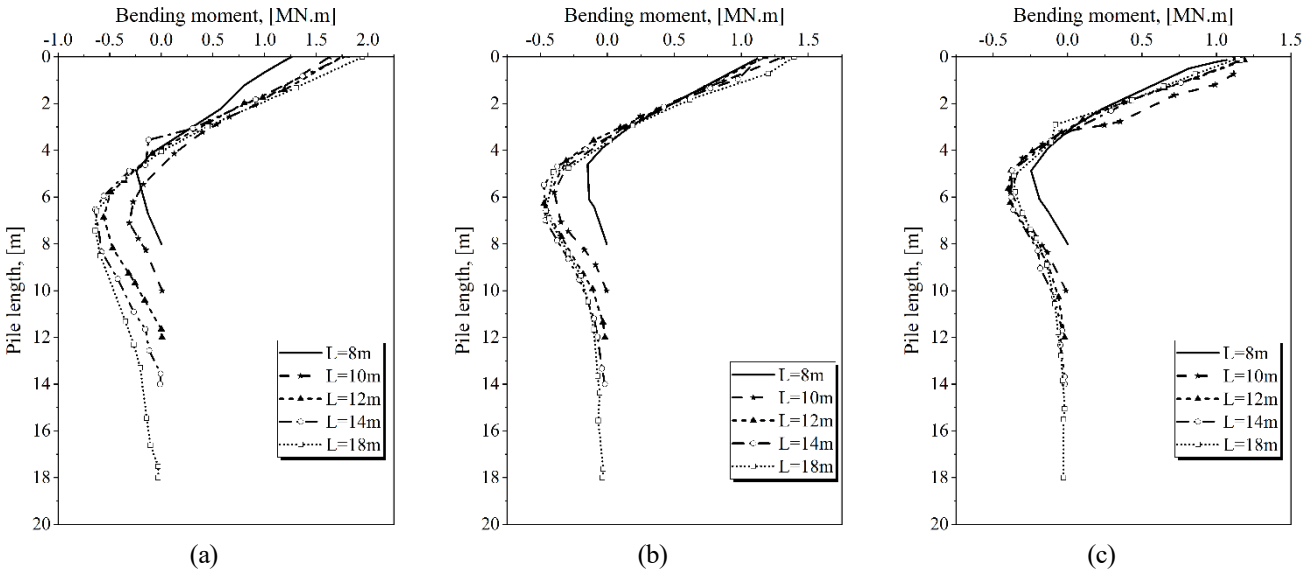


Fig. 21 Comparison of the bending moment along pile with change in pile length in: (a) loose, (b) medium density, and (c) high density sandy soil at the fixed pile head

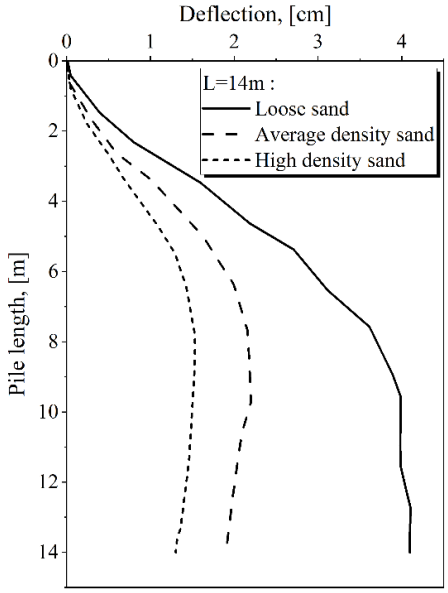


Fig. 22 Comparison of the effect of soil density on lateral pile displacement in the fixed head pile

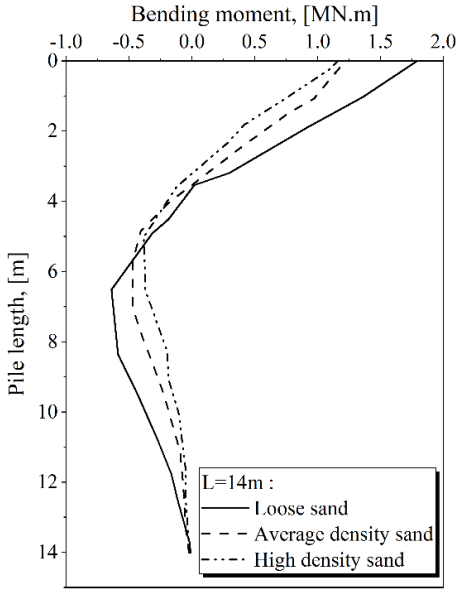


Fig. 23 Comparison of the effect of soil density on bending moment in the fixed head pile

more force and moment.

• With increasing sandy soil density, the lateral displacement of the pile head and the maximum bending moment is reduced. This is because with increasing soil density, the hardness and strength of the soil increases and the soil slope become more stable, and the soil grains cannot move easily as loose sandy soils, resulting in less bending moment and deformation applied to the pile. As a result, dense sandy soils have higher shear strength due to more locking between the soil grains, and the soil grains cannot move freely and easily.

• As the $S/D$ ratio increases, the lateral displacement of the piles decreases. This is because as the $S/D$ ratio decreases, the behavior of the piles becomes more like that of continuous aggregates. As the $S/D$ ratio increases, the bending moment in a pile is increased, and the position of the maximum bending moment goes up and is located in the upper half of the pile; In other words, as the $S/D$ ratio increases, the maximum amount of bending moment increases and the depth decreases. This is because the load area of each pile, which is affected by the lateral displacement of the soil, has expanded with an increasing $S/D$ ratio.

• In the case of a fixed pile head, with increasing $L$, the amount of bending moment at the pile head in all three types of soil has gradually increased. As observed, increasing the $L$ has very little effect on increasing the amount of bending moment. As a result, a very small

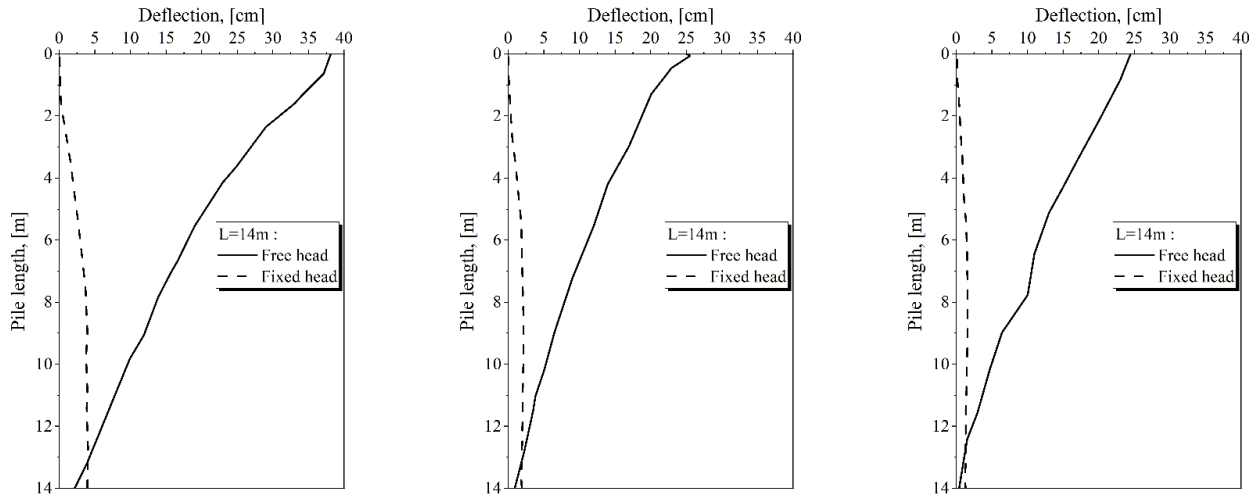


Fig. 24 Comparison of the effect of pile head conditions on lateral displacement in: (a) loose, (b) medium density, and (c) high density sandy soil

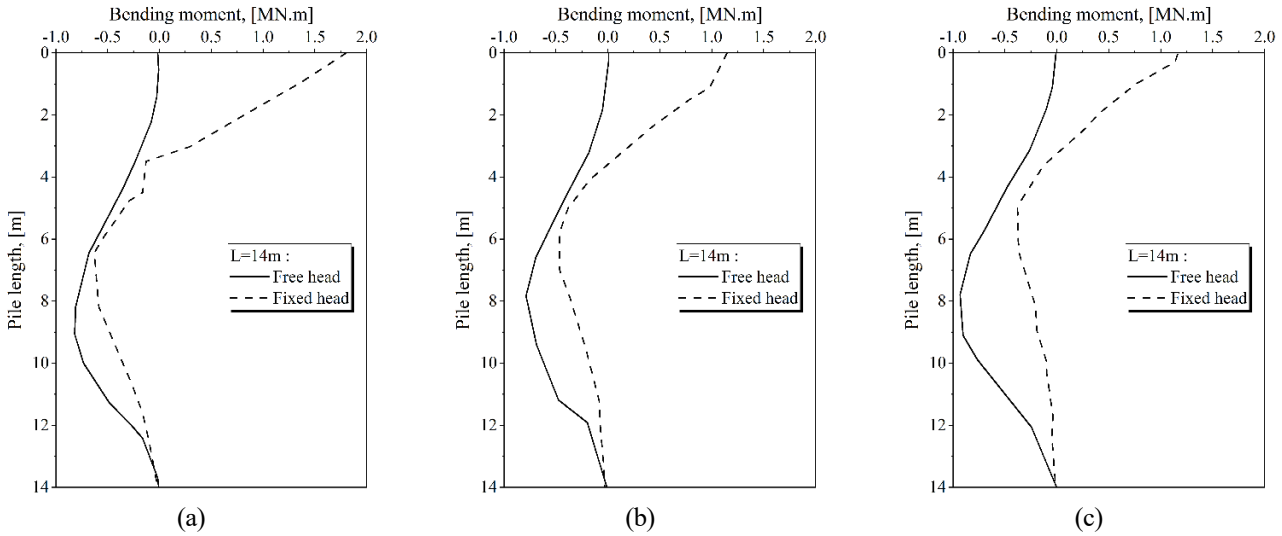


Fig. 25 Comparison of the effect of pile head conditions on bending moment in: (a) loose, (b) medium density, and (c) high density sandy soil

increase of approximately 1.2 times the maximum bending moment is achieved by doubling *L* used.

• If the head of the pile is fixed, the maximum lateral displacement of the pile is reduced, and the maximum bending moment is increased due to the relative increase in lateral stiffness of the pile. The maximum bending moment in the fixed pile head position is above the pile, while the maximum bending moment in the free pile is approximately in the center of the pile. The greater the amount of bending moment at the shallow depths of the pile in the fixed pile head indicates the effect of the inertial force due to the structure on the pile performance.

## References

Alemdag, S., Akgun, A., Kaya, A. and Gokceoglu, C. (2014), "A large and rapid planar failure: causes, mechanism, and consequences (Mordut, Gumushane, Turkey)", *Arabian J. Geosci.*, **7**(3), 1205-1221. https://doi.org/10.1007/s12517-012-0821-1.

Aghayari Hir, M., Zaheri, M. and Rahimzadeh, N. (2022), "Prediction of rural travel demand by spatial regression and artificial neural network methods (Tabriz County)", *J. Transport. Res.*, https://doi.org/10.22034/TRI.2022.312204.2970.

Ausilio, E., Conte, E. and Dente, G. (2001), "Stability analysis of slopes reinforced with piles", *Comput. Geotech.*, **28**(8), 591-611. https://doi.org/10.1016/S0266-352X(01)00013-1.

Beer, E.E. and Wallays, M. (1972), "Forces induced in piles by unsymmetrical surcharges on the soil around the piles", *Proceedings of the 5th Eur Conf On Soil Proc/Sp/, Conf Paper*.

Benemaran, R.S. and Esmaeili-Falak, M. (2020), "Optimization of cost and mechanical properties of concrete with admixtures using MARS and PSO", *Comput. Concrete*, **26**(4), 309-316. https://doi.org/10.12989/cac.2020.26.4.309.

Briançon, L. and Simon, B. (2012), "Performance of pile-supported embankment over soft soil: Full-scale experiment", *J. Geotech. Geoenviron. Eng.*, **138**(4), 551-561.

https://doi.org/10.1061/(ASCE)GT.1943-5606.0000561.
Cai, F. and Ugai, K. (2000), "Numerical analysis of the stability of a slope reinforced with piles", *Soils Found.*, **40**(1), 73-84. https://doi.org/10.3208/sandf.40.73.
Chen, L.T. and Poulos, H.G. (1997), "Piles subjected to lateral soil movements", *J. Geotechn. Geoenviron. Eng.*, **123**(9), 802-811. https://doi.org/10.1061/(ASCE)1090-0241(1997)123:9(802).
Cheng, Y.M., Lansivaara, T. and Wei, W.B. (2007), "Two-dimensional slope stability analysis by limit equilibrium and strength reduction methods", *Comput. Geotech.*, **34**(3), 137-150. https://doi.org/10.1016/j.compgeo.2006.10.011.
Chow, Y.K. (1996), "Analysis of piles used for slope stabilization", *Int. J. Numer. Anal. Method. Geomech.*, **20**(9), 635-646. https://doi.org/10.1002/(SICI)1096-9853(199609)20:9<635::AID-NAG839>3.0.CO;2-X.
Dai, W., Jiang, P., Ding, J. and Fu, B. (2017), "The influence of strength reduction method on slope stability under different instability criteria", *Proceedings of the International Conference on Architectural Engineering and New Materials*.
Davies, J.P., Loveridge, F.A., Perry, J., Patterson, D. and Carder, D. (2003), *Stabilisation of a landslide on the M25 highway London's main artery*.
Dawson, E.M., Roth, W.H. and Drescher, A. (1999), "Slope stability analysis by strength reduction", *Géotechnique*, **49**(6), 835-840. https://doi.org/10.1680/geot.1999.49.6.835.
Demerdash, M.A. (1996), *An experimental study of piled embankments incorporating geosynthetic basal reinforcement*. Newcastle University. http://theses.ncl.ac.uk/jspui/handle/10443/309
Donald, I.B. andGiam, S.K. (1988), "Application of the nodal displacement method to slope stability analysis", *Proceedings of the Australia-New Zealand Conference on Geomechanics, 5th, 1988, Sydney*, *88/11*.
Esmaeili-Choobar, N., Esmaeili-Falak, M., Roohi-hir, M. and Keshtzad, S. (2013), "Evaluation of collapsibility potential at Talesh, Iran", *EJGE*, **18**, 2561-73.
Esmaeili-Falak, M. and Hajialilue-Bonab, M. (2012), "Numerical studying the effects of gradient degree on slope stability analysis using limit equilibrium and finite element methods", *Int. J. Academic Res.*, **4**(4), 216-222. https://doi.org/10.7813/2075-4124.2012/4-4/A.30
Esmaeili-Falak, M., Katebi, H., Vadiati, M. and Adamowski, J. (2019), "Predicting triaxial compressive strength and Young's modulus of frozen sand using artificial intelligence methods", *J. Cold Reg. Eng.*, **33**(3), 04019007. https://doi.org/10.1061/(ASCE)CR.1943-5495.0000188.
Esmaeili-Falak, M., Katebi, H. and Javadi, A. (2018), "Experimental study of the mechanical behavior of frozen soils-A case study of tabriz subway", *Periodica Polytechnica Civil Eng.*, **62**(1), 117-125. https://doi.org/10.3311/PPci.10960.
Esmaeili Falak, M. and Sarkhani Benemaran, R. (2022), "Investigating the stress-strain behavior of frozen clay using triaxial test", *J. Struct. Constr. Eng.*, 10.22065/JSCE.2022.332406.2747.
Fahimifar, A., Abdolmaleki, A. and Soltani, P. (2014), "Stabilization of rock slopes using geogrid boxes", *Arabian J. Geosci.*, **7**(2), 609-621. https://doi.org/10.1007/s12517-012-0755-7.
Fan, W., Wei, Y. and Deng, L. (2018), "Failure modes and mechanisms of shallow debris landslides using an artificial rainfall model experiment on Qin-ba mountain", *Int. J. Geomech.*, **18**(3), 4017157. https://doi.org/10.1061/(ASCE)GM.1943-5622.0001068.
Fang Pai, L. and Gang Wu, H. (2021), "Shaking table test of comparison and optimization of seismic performance of slope reinforcement with multi-anchor piles", *Soil Dynam. Earthq. Eng.*, **145**, 106737. https://doi.org/10.1016/j.soildyn.2021.106737
Fang Pai, L., Gang Wu, H., Guan, W., Wei, H. and Tang, L. (2022), "Shaking table test for seismic optimization of soil slope reinforced by new EPS pile under earthquake", *Soil Dynam. Earthq. Eng.*, **154**, 107140. https://doi.org/10.1016/j.soildyn.2021.107140.
Fukumoto, Y. (1972), "Study on the behaviour of stabilization piles for land-slides", *Soils Found.*, **12**(2), 61-73. https://doi.org/10.3208/sandf1972.12.61
Fukumoto, Y. (1976), "The behaviour of piles for preventing landslide", *Soils Found.*, ***16***(2), 91-103. https://doi.org/10.3208/sandf1972.16.2_91
Fukumoto, Y. (1975), "Experiment study on the behavior of lateral resistance of piles against a land-sliding.(1)", *Landslides*, **12**(1), 20-24. https://doi.org/10.3313/jls1964.12.20.
Fukuoka, M. (1977), "The effects of horizontal loads on piles due to landslides", *Proceedings of the 10th Spec. Session, 9th Int. Conf. on SMFE*.
Gao, Y.F., Zhang, F., Lei, G.H. and Li, D.Y. (2013), "An extended limit analysis of three-dimensional slope stability", *Géotechnique*, **63**(6), 518-524. https://doi.org/10.1680/geot.12.T.004.
Ge, D.M., Zhao, L.C. and Esmaeili-Falak, M. (2022), "Estimation of rapid chloride permeability of SCC using hyperparameters optimized random forest models", *J. Sustain. Cement-Based Mater.*, 1-19. https://doi.org/10.1080/21650373.2022.2093291.
Goh, A.T.C., Teh, C.I. and Wong, K.S. (1997), "Analysis of piles subjected to embankment induced lateral soil movements", *J. Geotech. Geoenviron. Eng.*, **123**(9), 792-801. https://doi.org/10.1061/(ASCE)1090-0241(1997)123:9(792).
Griffiths, D.V. and Lane, P.A. (2001), "Slope stability analysis by finite elements", *Geotechniq. London*, **51**(7), 653-654.
Hajiazizi, M., Bavali, M. and Fakhimi, A. (2018), "Numerical and experimental study of the optimal location of concrete piles in a saturated sandy slope", *Int. J. Civil Eng.*, **16**(10), 1293-1301. https://doi.org/10.1007/s40999-017-0155-1
Hajiazizi, M., Nasiri, M. and Mazaheri, A.R. (2017), "The effect of fixed piles tip on stabilization of earth slopes", *Scientia Iranica*, **25**(5), 2550-2560. https://doi.org/10.24200/sci.2017.4211.
Hassiotis, S., Chameau, J.L. and Gunaratne, M. (1997), "Design method for stabilization of slopes with piles", *J. Geotech. Geoenviron. Eng.*, **123**(4), 314-323. https://doi.org/10.1061/(ASCE)1090-0241(1997)123:4(314).
Hull, T.S., Lee, C.Y. andPoulos, H.G. (1991), *Mechanics of pile reinforcement for unstable slopes*, University of Sydney, School of Civil and Mining Engineering.
Itasca Consulting Group, I. (20125), *FLAC3D, Fast Lagrangian Analysis of Continue in 3Dimensions*.
Ito, T. and Matsui, T. (1975), "Methods to estimate lateral force acting on stabilizing piles", *Soils Found.*, **15**(4), 43-59. https://doi.org/10.3208/sandf1972.15.4_43.
Jeong, S., Kim, B., Won, J. and Lee, J. (2003), "Uncoupled analysis of stabilizing piles in weathered slopes", *Comput. Geotech.*, **30**(8), 671-682. https://doi.org/10.1016/j.compgeo.2003.07.002.
Jiang, J., Zhao, Q., Jiang, H., Wu, Y. and Zheng, X. (2022), "Stability evaluation of finite soil slope in front of piles in landslide with displacement-based method", *Landslides*, **19**(11), 2653-2669.
Kourkoulis, R., Gelagoti, F., Anastasopoulos, I. and Gazetas, G. (2011), "Slope stabilizing piles and pile-groups: Parametric study and design insights", *J. Geotech. Geoenviron. Eng.*, **137**(7), 663-677. https://doi.org/10.1061/(ASCE)GT.1943-5606.0000479.
Lei, H., Liu, X., Song, Y. and Xu, Y. (2021), "Stability analysis of slope reinforced by double-row stabilizing piles with different locations", *Nat. Hazards*, **106**(1), 19-42. https://doi.org/10.1007/s11069-020-04446-2.

Li, Z. and Xiao, S. (2022), "Seismic stability analysis of two-stage slopes reinforced with one row of piles", *Soil Dynam. Earthq. Eng.*, **153**, 107079. https://doi.org/10.1016/j.soildyn.2021.107079.

Matsui, T. andSan, K.C. (1992), "Finite element slope stability analysis by shear strength reduction technique", *Soils Found.*, **32**(1), 59-70. https://doi.org/10.3208/sandf1972.32.59.

Mohapatra, S.R., Rajagopal, K. and Sharma, J. (2016), "Direct shear tests on geosynthetic-encased granular columns", *Geotext. Geomembranes*, **44**(3), 396-405. https://doi.org/10.1016/j.geotexmem.2016.01.002.

Moradi, G., Hassankhani, E. and Halabian, A.M. (2022), "Experimental and numerical analyses of buried box culverts in trenches using geofoam", *Proceedings of the Institution of Civil Engineers-Geotechnical Engineering*, **175**(3), 311-322.

Naylor, D.J. (1982), "Finite elements and slope stability", *Numerical Method. Geomech.*, 229-244. https://doi.org/10.1007/978-94-009-7895-9_10

Oakland, M.W. and Chameau, J.A. (1984), "Finite-element analysis of drilled piers used for slope stabilization", In *Laterally loaded deep foundations: Analysis and performance*. ASTM International.

Peng, W., Zhao, M., Zhao, H. and Yang, C. (2022), "Seismic stability of the slope containing a laterally loaded pile by finite-element limit analysis", *Int. J. Geomech.*, **22**(1), 06021033. https://doi.org/10.1061/(ASCE)GM.1943-5622.0002226.

Polysou, N.C., Coulter, T.S. and Sobkowicz, J.C. (1998), "Design, construction and performance of a pile wall stabilizing a landslide", *Proceedings of the 51th Can Geotech Conference*.

Poorjafar, A., Esmaeili-Falak, M. andKatebi, H. (2021), "Pile-soil interaction determined by laterally loaded fixed head pile group", *Geomech. Eng.*, **26**(1), 13-25. https://doi.org/10.12989/gae.2021.26.1.013.

Poulos, H.G. and Chen, L.T. (1997), "Pile response due to excavation-induced lateral soil movement", *J. Geotech. Geoenviron. Eng.*, **123**(2), 94-99. https://doi.org/10.1061/(ASCE)1090-0241(1997)123:2(94).

Poulos, H.G. (1995), "Design of reinforcing piles to increase slope stability", *Can. Geotech. J.*, **32**(5), 808-818. https://doi.org/10.1139/t95-078.

Reese, L.C. and Van Impe, W.F. (2000), *Single piles and pile groups under lateral loading*. CRC press.

Sarkar, K., Singh, T.N. and Verma, A.K. (2012), "A numerical simulation of landslide-prone slope in Himalayan region—a case study", *Arabian J. Geosci.*, **5**(1), 73-81. https://doi.org/10.1007/s12517-010-0148-8.

Sarkhani Benemaran, R., Esmaeili-Falak, M. and Katebi, H. (2021), "Physical and numerical modelling of pile-stabilised saturated layered slopes", *Proceedings of the Institution of Civil Engineers: Geotechnical Engineering*, 1-16. https://doi.org/10.1680/jgeen.20.00152.

Sarkhani Benemaran, R., Esmaeili-Falak, M. and Javadi, A. (2022), "Predicting resilient modulus of flexible pavement foundation using extreme gradient boosting based optimised models", *Int. J. Pavement Eng.*, 1-20. https://doi.org/10.1080/10298436.2022.2095385.

Sharafi, H. and Sojoudi, Y. (2016), "Experimental and numerical study of pile-stabilized slopes under surface load conditions", *Int. J. Civil Engi.*, **14**(4), 221-232. https://doi.org/10.1007/s40999-016-0017-2.

Shi, X., Yu, X. and Esmaeili-Falak, M. (2023), "Improved arithmetic optimization algorithm and its application to carbon fiber reinforced polymer-steel bond strength estimation", *Compos. Struct.*, **306**, 116599. https://doi.org/10.1016/j.compstruct.2022.116599.

Shooshpasha, I. and Amirdehi, H.A. (2015), "Evaluating the stability of slope reinforced with one row of free head piles", *Arabian J. Geosci.*, **8**(4), 2131-2141. https://doi.org/10.1007/s12517-014-1272-7.

Singh, T.N., Pradhan, S.P. and Vishal, V. (2013), "Stability of slopes in a fire-prone mine in Jharia Coalfield, India", *Arabian J. Geosci.*, **6**(2), 419-427. https://doi.org/10.1007/s12517-011-0341-4.

Sun, S.W., Wang, W. and Zhao, F. (2014), "Three-dimensional stability analysis of a homogeneous slope reinforced with micropiles", *Math. Probl. Eng.*, 1-11. https://doi.org/10.1155/2014/864017.

Tschebotarioff, G. (1973). *Foundations, retaining and earth structures-the art of design and construction and its scientific bases in soil mechanics*.

Ugai, K. and Leshchinsky, D. (1995), "Three-dimensional limit equilibrium and finite element analyses: A comparison of results", *Soils Found.*, **35**(4), 1-7. https://doi.org/10.3208/sandf.35.4_1.

Viggiani, C. (1981), "Ultimate lateral load on piles used to stabilize landslides", *Proceedings of the 10th Int. Conf. on SMFE*.

Wang, Y., Smith, J.V. and Nazem, M. (2021), "Optimisation of a slope-stabilisation system combining gabion-faced geogrid-reinforced retaining wall with embedded piles", *KSCE J. Civil Eng.*, **25**(12), 4535-4551. https://doi.org/10.1007/s12205-021-1300-6.

Wei, W.B. and Cheng, Y.M. (2009), "Strength reduction analysis for slope reinforced with one row of piles", *Comput. Geotech.*, **36**(7), 1176-1185. https://doi.org/10.1016/j.compgeo.2009.05.004.

Wei, W.B., Cheng, Y.M. and Li, L. (2009), "Three-dimensional slope failure analysis by the strength reduction and limit equilibrium methods", *Comput. Geotech.*, **36**(1-2), 70-80. https://doi.org/10.1016/j.compgeo.2008.03.003.

Won, J., You, K., Jeong, S. and Kim, S. (2005), "Coupled effects in stability analysis of pile–slope systems", *Comput.Geotech.*, **32**(4), 304-315. https://doi.org/10.1016/j.compgeo.2005.02.006.

Xu, C., Xue, L., Cui, Y., Guo, S., Zhai, M., Bu, F. and Chen, M.T. (2022), "A new multi-objective comprehensive optimization model for homogeneous slope reinforced by anti-slide piles: Insights from numerical simulation", *Lithosphere*, 2022(1). https://doi.org/10.2113/2022/6499724.

Yamin, M. (2007), *Landslide stabilization using a single row of rock-socketed drilled shafts and analysis of laterally loaded drilled shafts using shaft deflection data*. University of Akron.

Yang, S., Ren, X. and Zhang, J. (2011), "Study on embedded length of piles for slope reinforced with one row of piles", *J. Rock Mech. Geotech. Eng.*, **3**(2), 167-178. https://doi.org/10.3724/SP.J.1235.2011.00167.

Zeinkiewicz, O., Humpheson, C. and Lewis, R. (1975), "Associated and non-associated visco-plasticity in soils mechanics", *J. Geotech.*, **25**(5), 671-689.

Zeng, S. and Liang, R. (2002), "Stability analysis of drilled shafts reinforced slope", *Soils Found.*, **42**(2), 93-102. https://doi.org/10.3208/sandf.42.2_93.

Zienkiewicz, O.C., Humpheson, C. and Lewis, R.W. (1975), "Associated and non-associated visco-plasticity and plasticity in soil mechanics", *Geotechnique*, **25**(4), 671-689.

*GC*